Analysis and Solution for Operations of Overcurrent Relay in Wind Power System

Authors:

Yeonho Ok, Jaewon Lee, Jaeho Choi

Date Submitted: 2018-11-28

Keywords: coordination of protection relay, wind speed, malfunction of protection relay, wind power system, overcurrent relay

Abstract:

Wind power systems are being integrated increasingly into the power grid because of their large capacity and easy access to the transmission grid. The reliability of wind power plants is very important and the elimination of protective relay's malfunctions is essential to the mitigation of power quality problems due to the frequent starts and stops of high capacity wind generators. In this study, the problem of frequent false operations of the protective relays are analyzed using real data as line voltages, line currents, and wind speed. A new re-coordination of the overcurrent relay (OCR) based on the wind speed is proposed to avoid frequent operations of relays and tested for a grid-connected wind farm. This study verifies that the false actions by the OCRs that are not accompanied by actual electrical faults in the power grid or wind power system can be solved by the appropriate re-coordination of the OCR.

Record Type: Published Article

Submitted To: LAPSE (Living Archive for Process Systems Engineering)

Citation (overall record, always the latest version):	LAPSE:2018.1153
Citation (this specific file, latest version):	LAPSE:2018.1153-1
Citation (this specific file, this version):	LAPSE:2018.1153-1v1

DOI of Published Version: https://doi.org/10.3390/en9060458

energies

MDPI

Article

Analysis and Solution for Operations of Overcurrent Relay in Wind Power System

Yeonho Ok [1,2], Jaewon Lee [1] and Jaeho Choi [2,*]

[1] Research Institute, Power 21 Corporation, Daejeon 305-509, Korea; oyh@power21.co.kr (Y.O.); ljw@power21.co.kr (J.L.)

[2] School of Electrical Engineering, Chungbuk National University, Chungbuk 28644, Korea

* Correspondence: choi@cbnu.ac.kr; Tel.: +82-43-261-2425; Fax: +82-43-276-7217

Academic Editor: David Wood

Received: 1 February 2016; Accepted: 7 June 2016; Published: 16 June 2016

Abstract: Wind power systems are being integrated increasingly into the power grid because of their large capacity and easy access to the transmission grid. The reliability of wind power plants is very important and the elimination of protective relay's malfunctions is essential to the mitigation of power quality problems due to the frequent starts and stops of high capacity wind generators. In this study, the problem of frequent false operations of the protective relays are analyzed using real data as line voltages, line currents, and wind speed. A new re-coordination of the overcurrent relay (OCR) based on the wind speed is proposed to avoid frequent operations of relays and tested for a grid-connected wind farm. This study verifies that the false actions by the OCRs that are not accompanied by actual electrical faults in the power grid or wind power system can be solved by the appropriate re-coordination of the OCR.

Keywords: overcurrent relay; wind power system; malfunction of protection relay; wind speed; coordination of protection relay

1. Introduction

Wind power systems (WGSs) are connected to the power grid with ranges of voltages worldwide. Recently, with the increase of the installation of WGSs, the reliability of wind power systems has been treated as a very important issue in the power system technology. In wind power plants, protection with relays, such as overspeed, overcurrent, neutral overcurrent, under voltage, and phase asymmetry relays along with their operation have been studied. These relay operations are more frequent when the power plant is linked to the distribution system because the internal electrical problems in the distribution power lines affect the power plant directly. The literature was surveyed regarding the protective system when the wind generator turbine is linked to the distribution system. The protection and control of the wind power system linked to the power grid was considered [1–3]. The protection coordination when the fault occurs at the other feeder was studied [4]. Generally, the wind power system ought to be protected from lightning strikes [5] and the power distribution should be kept more flexible for relay setting to accept the network configuration and operational status of a WGS [6,7]. The protection in the case of short-circuit faults of the power grid was discussed [8–10]; the protection against the low voltage phenomenon occurring at the instant of a short-circuit or ground fault condition of the power system is described [11,12]; the crow-bar function inside the wind power system in the case of the power grid fault was studied [13–16]; and the internal direct current (DC) protection of the wind power system was reviewed [17–19]. On the other hand, most existing studies presented examples of the operation of protective relays without considering the wind speed. When the wind speed exceeds the reference wind speed, the protection strategy for a WGS should be designed considering the variation of the electrical characteristics of the WGS with the changes in

wind speed. The optimal model of the wind power system, whose output was changed by the wind speed, was discussed [20], and the impact of the power system due to a change in wind speed was reviewed [21,22]. Methods for controlling the output of the WGS when the wind speed exceeds the reference were reported [23–27]; the operation of an overspeed relay when the wind speed exceeds the reference velocity was proposed [28–30]; and the voltage variation according to the wind speed was discussed [31–33]. On the other hand, there is a paucity of studies of the operation of an overcurrent relay when the wind speed exceeds the reference wind speed.

Protective relays were often operated in the early days of the Sihwa wind power system, Korea. The phenomenon and operation of these protective relays was discussed generally [34]. In this paper, the problem and solution of the operation of protective relays is analyzed in detail using the measured line voltages, line currents, and wind speeds. Based on this analysis, the re-coordination of the overcurrent relay (OCR), considering the wind speed, is proposed to avoid the frequent operation of relays. This proposed procedure is tested practically at a real site. Through this study, it is verified that the OCR operates without any electrical faults in a power grid system or a wind power system, and this problem can be solved by the appropriate re-coordination of OCR. The cause of the relay operation is analyzed in Section 2, the OCR is re-coordinated to solve the problem in Section 3, and it is applied to the field and the four-month test results are illustrated as verification of the applied technology in Section 4.

2. Operation and Analysis of Overcurrent Relay

2.1. Installation and Operation of OCR

In South Korea, renewable energy generators (REGs) have generally been linked to the 22.9 kV distribution system. The power plant reviewed in this paper is the Sihwa wind power plant, which is currently under construction to be a microgrid. Figure 1 shows the single line diagram of the Sihwa wind power system with two wind power generators connected in parallel. The specifications of wind generator are followed as 1500 kW, 690 V, and 0.9 pf of a squirrel cage induction generator.

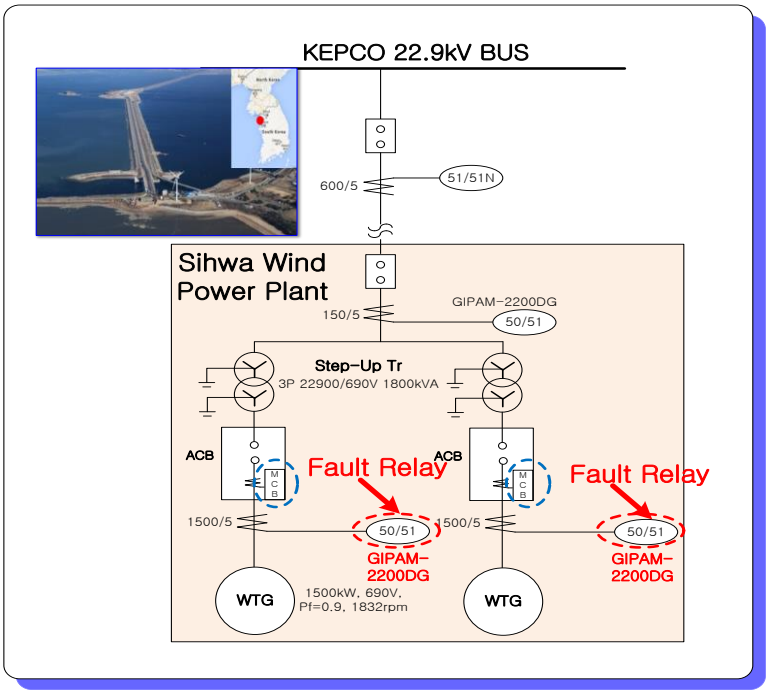

Figure 1. Single line diagram of Sihwa wind power system.

Two different types of digital composite relays were installed at each unit to protect the generators redundantly. One is the magnetic circuit breaker (MCB) relay provided by the generator manufacturer and the other is the digital integrated protection and monitoring equipment (GIPAM-2200DG) installed by the power plant operating company. During the generation of the wind turbine, the OCR(51) of GIPAM-2200DG operated frequently, whereas the MCB relay operated rarely and this discrepancy motivated our research to study a new re-coordination of the overcurrent relay (OCR).

The coordination of the OCR in a renewable energy system may be similar to that in general electric equipment; however, the time-delay OCR of this wind generator is often operated, as shown in Table 1. Such operation occurred 39 times for approximately 26 months at one unit. The minimum and maximum operating currents were 1788.5 A and 2316.7 A, respectively.

Table 1. Time delay operations of OCR* in GIPAM-2200DG**. Unit: A (Measured from 19 October 2011 to 29 December 2013).

No.	Fault	I_r	I_s	I_t	No.	Fault	I_r	I_s	I_t
1	R, S, T	1788.5	1863.8	1928.2	**21**	R, S, T	2123.1	2184.0	2257.7
2	R, S, T	1792.3	1874.0	1953.8	**22**	R, S, T	1920.5	1974.0	2057.7
3	R, S, T	2216.7	2263.5	2316.7	**23**	R, S, T	2002.6	2053.4	2155.1
4	R, S, T	2214.1	2283.9	2285.9	**24**	R, S, T	2000.0	2025.2	2100.0
5	R, S, T	2034.6	2091.8	2125.6	**25**	R, S, T	1944.9	2000.9	2073.1
6	R, S, T	2210.3	2250.6	2285.9	**26**	R, S, T	2030.8	2081.6	2137.2
7	R, S, T	2132.1	2189.2	2205.1	**27**	R, S, T	1985.9	2026.5	2091.0
8	R, S, T	2052.6	2117.4	2146.2	**28**	R, S, T	2023.1	2045.7	2093.6
9	R, S, T	1878.2	1924.0	1998.7	**29**	R, S, T	1925.6	1944.5	1997.4
10	R, S, T	2133.3	2208.4	2288.5	**30**	R, S, T	1970.5	1995.7	2059.0
11	R, S, T	2091.0	2144.3	2188.5	**31**	R, S, T	2042.3	2061.1	2123.1
12	R, S, T	1928.2	1997.0	2057.7	**32**	R, S, T	1974.4	1984.2	2080.8
13	R, S, T	1941.0	1985.5	2057.7	**33**	R, S, T	2069.2	2095.6	2189.7
14	R, S, T	1984.6	2035.4	2057.7	**34**	R, S, T	1909.0	1930.4	2028.2
15	R, S, T	1964.1	2016.2	2070.5	**35**	R, S, T	2223.1	2223.7	2294.9
16	R, S, T	2053.8	2116.1	2167.9	**36**	R, S, T	1997.4	2000.9	2062.8
17	R, S, T	2039.7	2080.3	2109.0	**37**	R, S, T	2029.5	2025.2	2091.0
18	R, S, T	2048.7	2085.4	2120.5	**38**	R, S, T	2026.9	2053.4	2155.1
19	R, S, T	2025.6	2068.7	2098.7	**39**	R, S, T	2059.0	2072.6	2125.6
20	R, S, T	2259.0	2308.3	2326.9					

OCR*: Over current relay; GIPAM-2200DG**: Digital integrated protection and monitoring equipment.

2.2. Analysis of OCR Operations

The time delay OCR may operate in an unbalanced load conditions or a short circuit accident, and may occur by a malfunction. Figure 2 illustrates the relay operating points in the OCR coordination curve. The relay operation does not appear to malfunction because they are placed on the right side of the OCR coordination curve.

The unbalanced ratio of the operating current of time-delay OCR is defined as:

$$\%\text{Unbalance} = \frac{Phase\ current}{\frac{\sum 3\ Phase\ current}{3}} \times 100 \quad (1)$$

The most serious unbalance ratio in Table 1 is R-phase 95.7% and T-phase 104.3% of No. 2. On the other hand, this is in the 35% acceptable range of the unbalance ratio for the distribution system in Korea; hence, time-delay OCR operations are not caused by an unbalance fault. If a short circuit fault occurs in the power grid or inside the power plant, the generator voltage falls and a voltage sag phenomenon occurs. As shown in Table 2, the minimum generator voltage when the time-delay OCR

operates is the R-phase voltage, 332.2 V (0.834 pu) of No. 38, which is higher than the setting value of low-voltage relay, 0.8 pu.

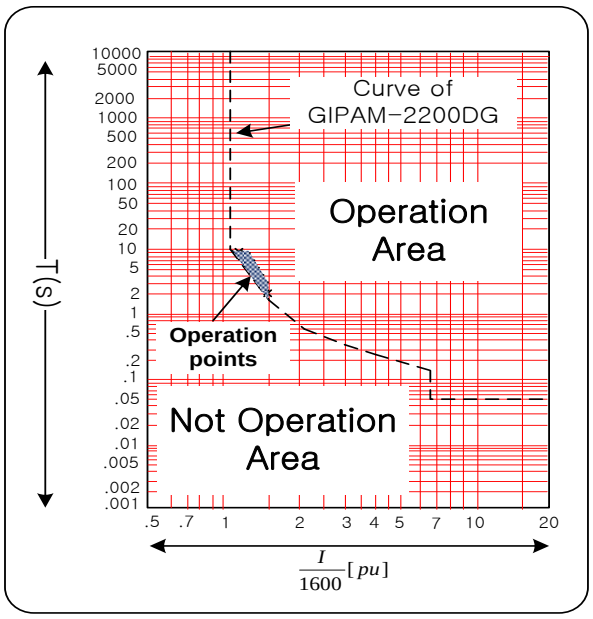

Figure 2. Relay operating points in OCR (over current relay) coordination curve.

Table 2. Generator voltages at the time of delay OCR operation.

Event No.	Phase Voltage (*V*)			Event No.	Phase Voltage (*V*)		
	V_r	V_s	V_t		V_r	V_s	V_t
1	359.6	369.9	361.4	**21**	366.8	375.3	369.2
2	358.4	369.0	359.8	**22**	368.4	377.1	371.0
3	368.4	372.6	369.7	**23**	364.8	375.1	369.2
4	373.6	376.0	371.5	**24**	382.2	387.7	383.8
5	378.3	382.3	378.0	**25**	373.8	381.8	375.3
6	369.3	372.2	368.4	**26**	370.4	376.7	371.3
7	377.4	380.3	375.5	**27**	373.1	378.9	374.4
8	370.6	375.5	369.5	**28**	385.3	387.7	385.4
9	372.5	381.2	376.0	**29**	383.5	386.8	384.5
10	357.5	368.4	360.9	**30**	386.9	392.4	388.8
11	374.0	379.6	374.6	**31**	376.8	382.3	376.9
12	360.5	369.9	362.7	**32**	367.7	376.7	370.8
13	373.8	381.4	376.4	**33**	362.3	372.0	365.0
14	376.5	379.1	375.1	**34**	367.5	377.1	370.4
15	372.2	378.5	373.1	**35**	347.1	353.5	372.2
16	375.2	382.3	376.0	**36**	351.7	359.1	378.2
17	390.5	393.3	389.9	**37**	351.2	358.0	374.0
18	383.5	386.3	382.9	**38**	332.2	343.2	364.8
19	379.7	382.1	378.2	**39**	358.7	368.8	372.4
20	375.4	377.1	373.3				

Therefore, the time-delay OCR operations are not caused by a short-circuit fault because the low-voltage relay does not operate when the time-delay OCR operates. The reference wind speed of the Sihwa wind power system is 12.5 m/s, and the output is 1500 kW. If the wind speed of the wind power system is faster than the reference wind speed and the output exceeds the rated output, the output should be limited to 1500 kW by adjusting the blade angle through the pitch control system. On

the other hand, the response of the speed control is limited due to the mechanical time constant of the pitch control system. Therefore, when the wind speed increases abruptly, it is difficult to maintain the output at 1500 kW before the OCR operates. Table 3 lists the wind speeds at the time of OCR operation. The wind speed data of Table 3 do not exactly match the wind speed at the OCR operation time, as shown by the mean value for five minutes.

Table 3. Wind speed at the time of OCR operation.

Event No.	Wind Speed	Event No.	Wind Speed	Event No.	Wind Speed	Event No.	Wind Speed	Event No.	Wind Speed	Event No.	Wind Speed
1	12.7	**8**	12.1	**15**	12.8	**22**	13.5	**29**	13.1	**36**	10.7
2	13.3	**9**	12.4	**16**	10.6	**23**	11.8	**30**	14.1	**37**	15.9
3	12.0	**10**	12.7	**17**	12.6	**24**	13.2	**31**	11.5	**38**	13.8
4	15.5	**11**	12.9	**18**	9.8	**25**	10.4	**32**	8.9	**39**	12.6
5	14.3	**12**	12.7	**19**	12.3	**26**	11.4	**33**	10.4		
6	11.7	**13**	12.2	**20**	20.1	**27**	15.8	**34**	13.1		
7	12.2	**14**	13.4	**21**	13.7	**28**	9.2	**35**	11.9		

Table 4 lists the monthly average wind speed from 2011 to 2012. A comparison of Tables 3 and 4 shows that the wind speed at the time of OCR operation is two times faster than the monthly average wind speed. Therefore, when the wind speed increases suddenly, the OCR operates before lowering the output to 1500 kW. To solve these problems, the re-coordination to delay the OCR's operation is needed for the high wind speed.

Table 4. Monthly average wind speed from 2011 to 2012.

Month	Wind Speed (2011)	Wind Speed (2012)
January	5.1	4.7
February	3.5	5.0
March	5.8	5.7
April	4.6	5.2
May	4.3	3.4
June	3.9	3.5
July	3.7	3.8
August	3.0	5.1
September	4.1	4.1
October	3.9	4.8
November	4.6	6.1
December	5.0	5.3
Average	4.3	4.7

3. Re-Coordination of over Current Relay in GIPAM-2200DG

3.1. Present Coordination of OCR

Appendix presents the impedance map (Figure A1) and specifications for the coordination of OCR. As mentioned above, MCB and GIPAM-2200DG are installed to protect generators doubly. The inverse definite minimum time (IDMT) in IEC225 is used to coordinate the OCR of GIPAM-2200DG, which is illustrated as follows:

$$t\,(\mathrm{s}) = \mathrm{TMS} \times \left\{ \frac{k}{\left(\frac{I_f}{I_{pu}}\right)^a} + c \right\} \tag{2}$$

where

t = operating time for a constant current, I (seconds);

I_f = energizing current (amps);
I_{pu} = over current pick-up setting (amps);
TMS = time multiplier setting; and
k, a, c = constants defining curve.

If the VI (Very Inverse) curve is applied, the present coordination curve by calculation is illustrated as follows:

$$t\,(\mathrm{s}) = \mathrm{TMS} \times \left\{ \frac{k}{\left(\frac{I_f}{I_{pu}}\right)^a + c} \right\} = 0.05 \times \left\{ \frac{13.5}{\left(\frac{I_f}{1620}\right)^1 + 0} \right\} \tag{3}$$

Figure 3 presents the coordination curves of the relays to protect the generator. The actual operation for the MCB or GIPAM-2200 DG is the green curve in Figure 3 on a short-current fault of a 690 V line.

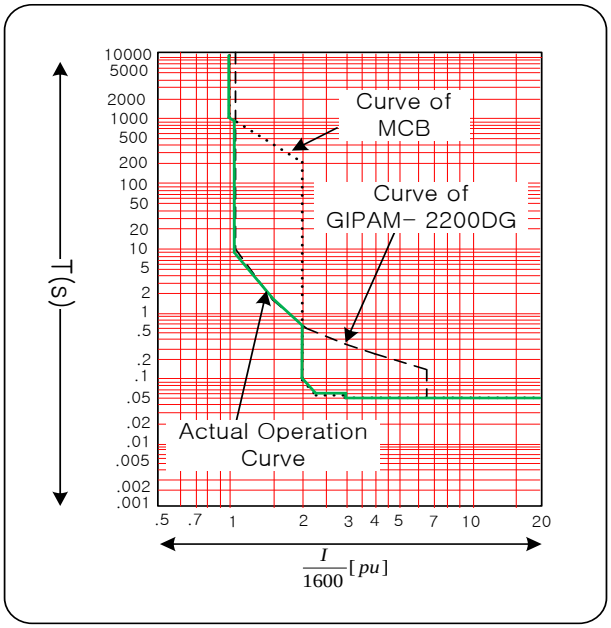

Figure 3. Present coordination curve of OCR for generator.

3.2. Power Factor in Coordination

In the case of the renewable energy system, the power factor is generally not considered to calculate the regulated current of generator. This is because the renewable energy sources, such as hydropower, solar power, etc., are unlikely to be overloaded without faults. On the other hand, because wind turbines operate at a power factor of 0.9 with wind gust conditions, the power factor should be taken into consideration for relay's setting values. Therefore, it is necessary to change the rated current of a wind power system from 1255 A to 1394 A, and the pick-up current from 1620 A to 1812 A as described in Equations (4) and (5):

$$I_{pu} = \frac{P}{\sqrt{3}V} \times 1.3 = \frac{1500 \times 10^3}{\sqrt{3} \times 690} \times 1.3 = 1620\ \mathrm{A} \tag{4}$$

$$I_{pu} = \frac{P}{\sqrt{3}V\cos\theta} \times 1.3 = \frac{1500 \times 10^3}{\sqrt{3} \times 690 \times 0.9} \times 1.3 = 1812\ \mathrm{A} \tag{5}$$

3.3. Lever of OCR in GIPAM-2200DG

The blade angle needs to be adjusted without the operation of an OCR as discussed above. The present time delay curve is VI (Very Inverse), but it is necessary to change it close to EI (Extremely Inverse).

Table 5 lists the operation time according to the lever of GIPAM-2200DG for the maximum, minimum and average values of the operation current.

Table 5. Operation time according to lever of GIPAM-2200DG.

GIPAM-2200DG	Lever	Operation Time		
		Minimum Operating Current 1788.5 A	**Average Operating Current 2052.6 A**	**Maximum Operating Current 2316.7 A**
Before change	0.05	6.49	2.53	1.57
After change	0.06	∞	6.10	2.91
	0.07	∞	7.12	3.39
	0.08	∞	8.13	3.88
	0.09	∞	9.15	4.36
	0.10	∞	10.17	4.85
	0.11	∞	11.18	5.33
	0.12	∞	12.20	5.82
	0.13	∞	13.22	6.30
	0.14	∞	14.23	6.79
	0.15	∞	15.25	7.27
	0.16	∞	16.27	7.75
	0.17	∞	17.28	8.24
	0.18	∞	18.30	8.72
	0.19	∞	19.32	9.21
	0.20	∞	20.33	9.69

The blade angle adjustment speed of the pitch control system, 2 °/s and Table 5 are considered synthetically, and the lever is then changed from 0.05 to 0.15 finally. The re-coordinated curve is the same as that expressed in Equation (6):

$$t\,(\mathrm{s}) = \mathrm{TMS} \times \left\{ \frac{k}{\left(\frac{I_f}{I_{pu}}\right)^a + c} \right\} = 0.15 \times \left\{ \frac{13.5}{\left(\frac{I_f}{1812}\right)^1 + 0} \right\} \quad (6)$$

Through the lever change, the wind power system can reserve the time to adjust the blade angle without the operation of the OCR under momentary gust conditions. Figure 4 presents graphs before and after reflecting the power factor and lever.

According to Table 5, although the current is increased to 2316.7 A during the situation of a wind gust, it provides a margin of 5.7 s to adjust the blade angle and reduce the incidence of false tripping. Figure 5 presents the MCB curve and GIPAM2200-DG curve after re-coordination. The actual operation curve of the OCR after re-coordination is shown in blue in this figure.

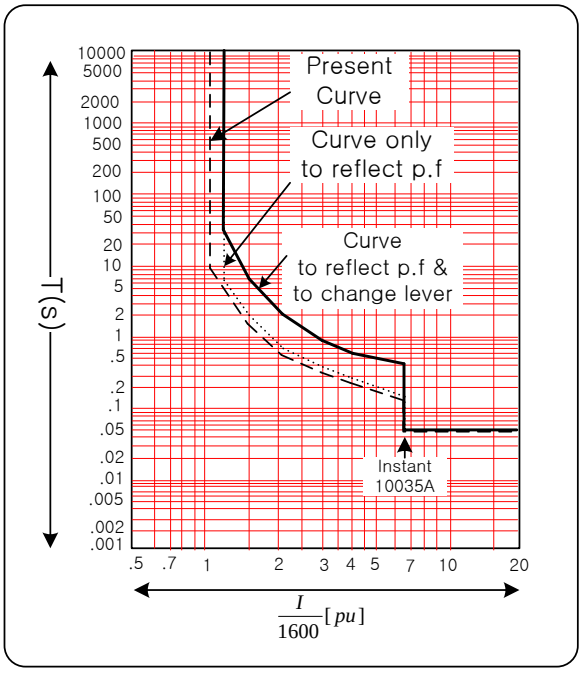

Figure 4. Curves before and after reflecting power factor (pf) and lever.

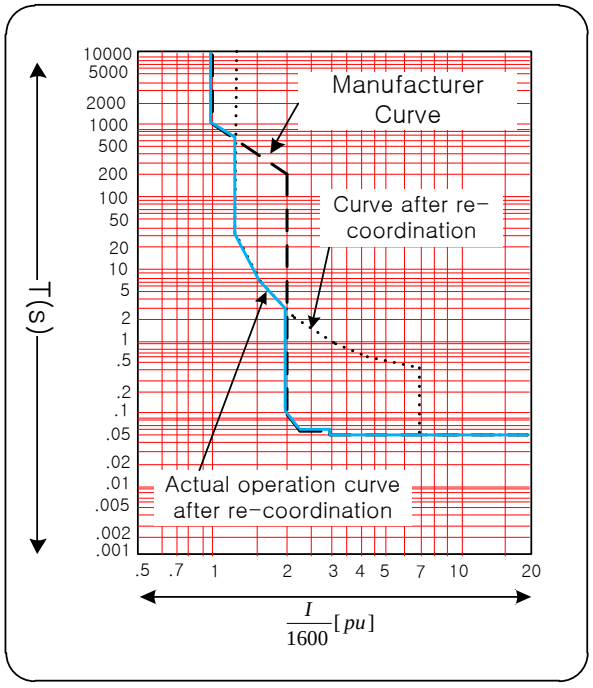

Figure 5. Re-coordination curve of the OCR for generator.

3.4. Problem and Solution of Re-Coordination

The actual OCR operation curves of the generator side after and before re-coordination are determined, as shown in Figure 6.

Figure 6 shows that it is beneficial to maintain the margin to adjust the blade angle and reduce the number of generator fault occurrences when the wind speed is faster than the reference wind speed.

On the other hand, when the wind speed is lower than the reference wind speed, an unprotected zone appears even under a short circuit fault condition, as shown in Figure 6.

To remove this unprotected zone, two protection curves according to the wind speed were applied. An anemometer installed upon review of the wind power plant was used. If the wind speed is faster than 13 m/s for 10 s continuously considering the pitch control speed and delay characteristics of protection relay, the setting of the protective relay is converted. If the wind speed is slower than 12 m/s during 10 s continuously, the setting of the protective relay is returned. Figure 7 shows the above settings.

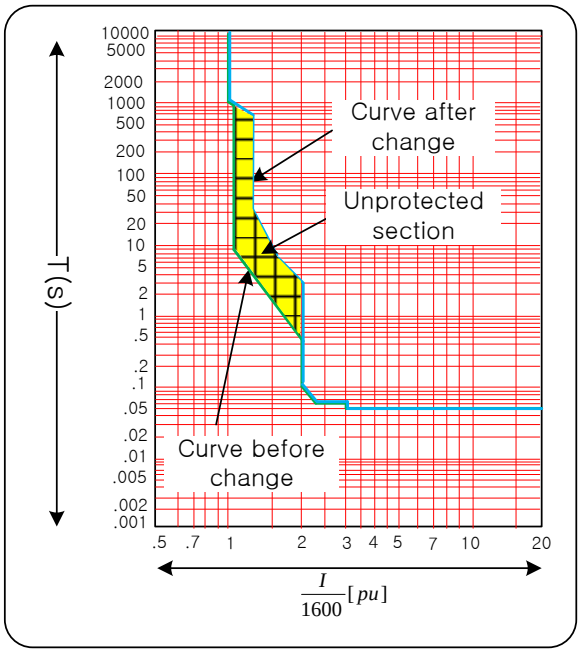

Figure 6. Actual OCR curves after and before re-coordination.

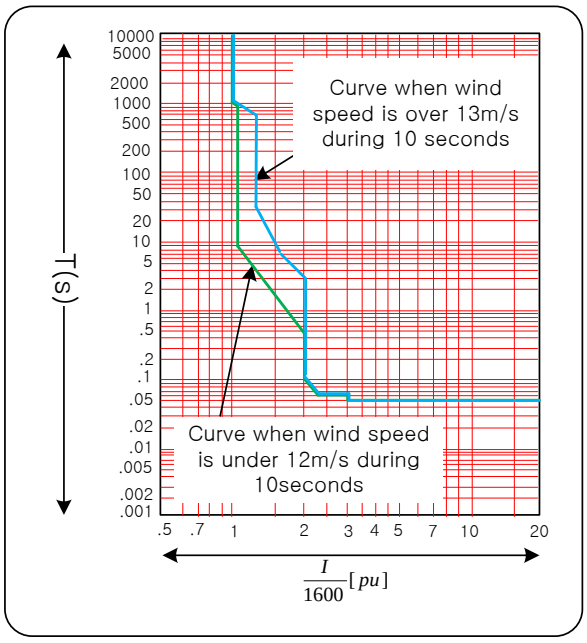

Figure 7. Final coordination of OCR.

4. Demonstration in the Field

The OCR of generator side is re-coordinated, as shown in Figure 7. The re-coordinated curve for the wind power plant of Sihwa Lake Microgrid system in Figure 8 was applied to the test from 5 March to 25 June 2014. Figure 8 presents the averaged wind speed data for 5 min over a 112 day period. The minimum wind speed at the instant of OCR operation, 8.9 m/s, which is illustrated in Table 3, is shown as the red line.

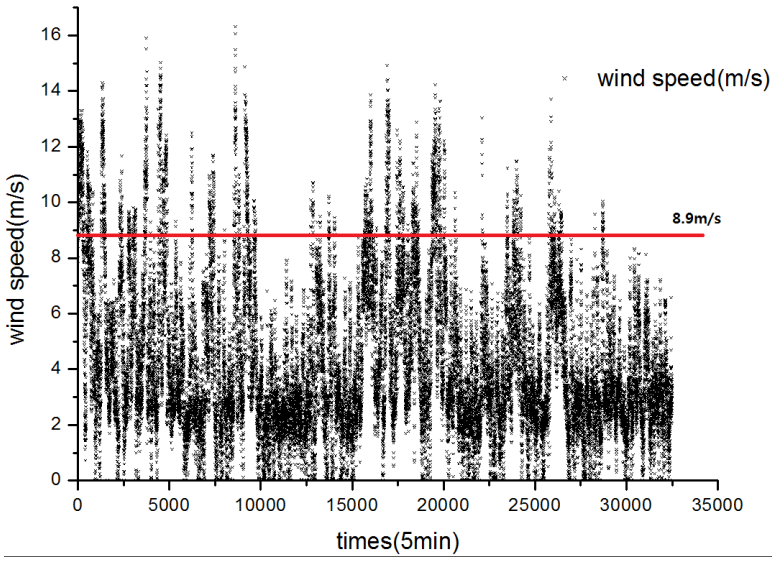

Figure 8. Wind speed during test.

During the test period, the wind speed data, which is faster than the minimum wind speed, 8.9 m/s, are illustrated in Table 6. The total number of cases faster than the minimum wind speed is 2479, which may have a high enough potential to operate the OCR before re-coordination, but there is no operation of the OCR during that period, and it is verified that the re-coordination of the OCR is appropriate for solving the problem of the frequent operation of the OCR.

Table 6. Wind speed during test.

Wind Speed (m/s)	Times	Operation	Remarks
Higher than 17.00	1	X	
16.00~16.99	2	X	
15.00~15.99	5	X	
14.00~14.99	35	X	O: Operation
13.00~13.99	119	X	X: No operation
12.00~12.99	320	X	Test Period:
11.00~11.99	422	X	5 March–25 June 2014
10.00~10.99	575	X	
8.90~9.99	1000	X	
Total	2479		

5. Conclusions

This paper reported the results of a case study on the operation of OCR in a wind power system. From the analysis based on the present coordination of the OCR, it is found that the frequent operation of OCR is not originated in the OCR's malfunctions. After considering the electrical faults and the wind speed, the further study of OCR operation shows that these erroneous overload faults, which cause OCR operations, are caused by wind gusts.

The OCR operated 39 times for 26 months in the Sihwa Lake Microgrid system, as shown in Table 1. To solve this problem, the re-coordination of the OCR according to the wind speed was performed through on-site tests, and it resulted in successful wind power generation without OCR operations for 112 days. In conclusion, the OCR for a wind power system should be coordinated differently from that of other renewable energy sources.

Acknowledgments: This study was supported by the KETEP (Korea Institute of Energy Technology Evaluation and Planning) through the (*Development for Microgrid Common Platform Technology, 20141010501870*) project.

Author Contributions: Yeonho Ok and Jaewon Lee conceived and designed the tests; Yeonho Ok and Jaeho Choi analyzed the data and wrote the paper.

Conflicts of Interest: The authors declare no conflict of interest.

Appendix

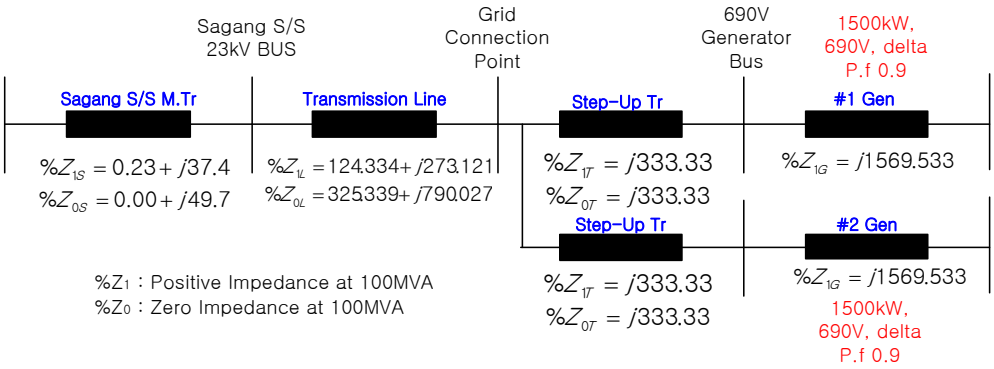

Figure A1. Impedance map.

References

1. Hornak, D.; Chau, N.H. Green power-wind generated protection and control considerations. In Proceedings of the 57th IEEE Annual Conference for Protective Relay Engineers, College Station, TX, USA, 1 April 2004; pp. 110–131.
2. Pradhan, A.K.; Joos, G. Adaptive distance relay setting for lines connecting wind farms. *IEEE Trans. Energy Convers.* **2007**, *22*, 206–213. [CrossRef]
3. Sujo, P.G.; Ashok, S. Malfunction of differential relays in wind farms. *Int. J. Adv. Electr. Electron. Eng.* **2014**, *3*, 27–31.
4. Wu, Y.K.; Lin, Z.T.; Lee, T.C.; Hsieh, T.Y.; Lin, W.M. Adaptive setting and simulation of distance protection relay in a long transmission system connected to an offshore wind farm. *J. Clean Energy Technol.* **2016**, *6*, 401–407. [CrossRef]
5. Glushakow, B. Effective lightning protection for wind turbine generators. *IEEE Trans. Energy Convers.* **2007**, *22*, 214–222. [CrossRef]
6. Yip, T.; An, C.; Lloyd, G.; Aten, M.; Ferri, B. Dynamic line rating protection for wind farm connections. In Proceedings of the 2009 CIGRE/IEEE PES Joint Symposium on Integration of Wide-Scale Renewable Resources into the Power Delivery System, Calgary, AB, Canada, 29–31 July 2009; pp. 1–5.
7. Altin, M.; Göksu, Ö.; Teodorescu, R.; Rodriguez, P.; Jensen, B.B.; Helle, L. Overview of recent grid codes for wind power integration. In Proceedings of the 12th IEEE International Conference on Optimization of Electrical and Electronic Equipment, Basov, Romania, 20–22 May 2010; pp. 1152–1160.
8. Sun, T.; Chen, Z.; Blaabjerg, F. Voltage recovery of grid-connected wind turbines with DFIG after a short-circuit fault. In Proceedings of the 35th IEEE Annual Power Electronics Specialists Conference, Aachen, Germany, 20–25 June 2004; Volume 3, pp. 1991–1997.

9. Erlich, I.; Bachmann, U. Grid code requirements concerning connection and operation of wind turbines in Germany. In Proceedings of the IEEE Power Engineering Society General Meeting, San Francisco, CA, USA, 12–16 June 2005; pp. 1253–1257.
10. Sun, T.; Chen, Z.; Blaabjerg, F. Transient stability of DFIG wind turbines at an external short-circuit fault. *Wind Energy* **2005**, *8*, 345–360. [CrossRef]
11. Lopez, J.; Sanchis, P.; Roboam, X.; Marroyo, L. Dynamic behavior of the doubly fed induction generator during three-phase voltage dips. *IEEE Trans Energy Convers.* **2007**, *22*, 709–717. [CrossRef]
12. Erlich, I.; Winter, W.; Dittrich, A. Advanced grid requirements for the integration of wind turbines into the German transmission system. In Proceedings of the IEEE Power Engineering Society General Meeting, Montreal, QC, Canada, 18–22 June 2006; pp. 1–7.
13. Chen, Z.; Guerrero, J.M.; Blaabjerg, F. A review of the state of the art of power electronics for wind turbines. *IEEE Trans. Power Electron.* **2009**, *24*, 1859–1875. [CrossRef]
14. Seman, S.; Niiranen, J.; Kanerva, S.; Arkkio, A.; Saitz, J. Performance study of a doubly fed wind-power induction generator under network disturbances. *IEEE Trans. Energy Convers.* **2006**, *21*, 883–890. [CrossRef]
15. Brochu, J.; Larose, C.; Gagnon, R. Validation of single-and multiple-machine equivalents for modeling wind power plants. *IEEE Trans. Energy Convers.* **2011**, *26*, 532–541. [CrossRef]
16. Morren, J.; De Haan, S.W. Short-circuit current of wind turbines with doubly fed induction generator. *IEEE Trans. Energy Convers.* **2007**, *22*, 174–180. [CrossRef]
17. Yang, J.; Fletcher, J.E.; O'Reilly, J. Multiterminal DC wind farm collection grid internal fault analysis and protection design. *IEEE Trans. Power Deliv.* **2010**, *25*, 2308–2318. [CrossRef]
18. Chen, Y.M.; Cheng, C.S.; Wu, H.C. Grid-connected hybrid PV/wind power generation system with improved DC bus voltage regulation strategy. In Proceedings of the 12th IEEE Applied Power Electronics Conference and Exposition, Dallas, TX, USA, 19–23 March 2006; pp. 1–7.
19. Erlich, I.; Wrede, H.; Feltes, C. Dynamic behavior of DFIG-based wind turbines during grid faults. In Proceedings of the Power Conversion Conference-Nagoya, Nagoya, Japan, 2–5 April 2007; pp. 1195–1200.
20. Lei, Y.; Mullane, A.; Lightbody, G.; Yacamini, R. Modeling of the wind turbine with a doubly fed induction generator for grid integration studies. *IEEE Trans. Energy Convers.* **2006**, *21*, 257–264. [CrossRef]
21. Banakar, H.; Luo, C.; Ooi, B.T. Impacts of wind power minute-to-minute variations on power system operation. *IEEE Trans. Power Syst.* **2008**, *23*, 150–160. [CrossRef]
22. Jauch, C.; Sørensen, P.; Norheim, I.; Rasmussen, C. Simulation of the impact of wind power on the transient fault behavior of the Nordic power system. *Electr. Power Syst. Res.* **2007**, *77*, 135–144. [CrossRef]
23. Erlich, I.; Kretschmann, J.; Fortmann, J.; Mueller-Engelhardt, S.; Wrede, H. Modeling of wind turbines based on doubly-fed induction generators for power system stability studies. *IEEE Trans. Power Syst.* **2007**, *22*, 909–919. [CrossRef]
24. Slootweg, J.G.; De Haan, S.W.H.; Polinder, H.; Kling, W.L. General model for representing variable speed wind turbines in power system dynamics simulations. *IEEE Trans. Power Syst.* **2003**, *18*, 144–151. [CrossRef]
25. Qiao, W.; Zhou, W.; Aller, J.M.; Harley, R.G. Wind speed estimation based sensorless output maximization control for a wind turbine driving a DFIG. *IEEE Trans. Power Electron.* **2008**, *23*, 1156–1169. [CrossRef]
26. Lo, K.Y.; Chen, Y.M.; Chang, Y.R. MPPT battery charger for stand-alone wind power system. *IEEE Trans. Power Electron.* **2011**, *26*, 1631–1638. [CrossRef]
27. Luo, C.; Banakar, H.; Shen, B.; Ooi, B.T. Strategies to smooth wind power fluctuations of wind turbine generator. *IEEE Trans. Energy Convers.* **2007**, *22*, 341–349. [CrossRef]
28. Li, P.; Banakar, H.; Keung, P.K.; Far, H.G.; Ooi, B.T. Macromodel of spatial smoothing in wind farms. *IEEE Trans. Energy Convers.* **2007**, *22*, 119–128. [CrossRef]
29. Thet, A.K.; Saitoh, H. Pitch control for improving the low-voltage ride-through of wind farm. In Proceedings of the Transmission and Distribution Conference and Exposition: Asia and Pacific, Seoul, Korea, 26–30 October 2009; pp. 1–4.
30. Dubey, R.; Samantaray, S.R.; Panigrahi, B.K. Adaptive distance protection scheme for shunt-FACTS compensated line connecting wind farm. *J. IET Gener. Transm. Distrib.* **2016**, *10*, 247–256. [CrossRef]
31. Haque, M.E.; Negnevitsky, M.; Muttaqi, K.M. A novel control strategy for a variable-speed wind turbine with a permanent-magnet synchronous generator. *IEEE Trans. Ind. Appl.* **2010**, *46*, 331–339. [CrossRef]
32. Pannell, G.; Atkinson, D.J.; Zahawi, B. Minimum-threshold crowbar for a fault-ride-through grid-code-compliant DFIG wind turbine. *IEEE Trans. Energy Convers.* **2010**, *25*, 750–759. [CrossRef]

33. Muyeen, S.M.; Takahashi, R.; Murata, T.; Tamura, J. A variable speed wind turbine control strategy to meet wind farm grid code requirements. *IEEE Trans. Power Syst.* **2010**, *25*, 331–340. [CrossRef]
34. Ok, Y.; Lee, J.; Choi, J. Coordination of over current relay for sudden rise of input energy in renewable power system. In Proceedings of the International Conference on Renewable Energy Research and Applications, Palermo, Italy, 22–25 November 2015; pp. 654–658.